

Spin Precession and Oscillations in Mesoscopic Systems

Martin Y. Veillette,* Cristina Bena,† and Leon Balents‡

Department of Physics, University of California at Santa Barbara, Santa Barbara, CA-93106

(Dated: November 10, 2018)

We compare and contrast magneto-transport oscillations in the fully quantum (single-electron coherent) and classical limits for a simple but illustrative model. In particular, we study the induced magnetization and spin current in a two-terminal double-barrier structure with an applied Zeeman field between the barriers and spin disequilibrium in the contacts. Classically, the spin current shows strong tunneling resonances due to spin precession in the region between the two barriers. However, these oscillations are distinguishable from those in the fully coherent case, for which a proper treatment of the electron phase is required. We explain the differences in terms of the presence or absence of coherent multiple wave reflections.

PACS numbers: 73.23.-b,42.25.Kb

I. INTRODUCTION

The recent progress in controlling and manipulating spins in semiconductors has attracted considerable interest in the prospect of developing electronics based on spin degrees of freedom^{1,2}. Numerous recent magneto-transport experiments expose “spin coherence” in the sense of long-lived oscillatory phenomena associated with spin precession^{3,4}. Some such oscillations, however, are expected to persist even in the classical limit as a consequence only of (approximate) spin-rotational invariance. The aim of this paper is to compare and contrast spin transport in simple models of classical and truly single-electron phase coherent conductors. We also give a set of general hydrodynamic transport equations that apply in the classical regime – and can be applied for quantitative modeling of a variety of experimental geometries.

Theoretically, although the electron spin is a quantum object at heart, its quantum nature has been largely ignored in studies of semiconductor spin transport. Most approaches are based on a semi-classical Boltzmann formalism, in which quantum mechanical effects appear only in the calculation of scattering rates and Fermi occupation factors^{5,6}. The resulting semi-classical transport equations were successfully applied in analyzing spin injection into semiconductors and in studying spin-polarized transport in inhomogeneous doped semiconductors^{7,8}. This approach essentially ignores all quantum interference effects, and is expected to hold when the inelastic mean free path is sufficiently short – i.e. for not too low temperature and for large samples. However, experiments on mesoscopic conductors allow a detailed exploration of phase coherent phenomena, as has been amply demonstrated for charge transport.⁹

To search for single-electron spin coherence, it is crucial to have some idea of its distinguishing features.¹⁰ The search is complicated by the existence of essentially *classical* spin oscillations. In particular, in any system which, in absence of applied fields, can be approximated as spin-rotationally invariant, a continuity equation (modified by a precessional “mode-coupling” term) exists:

$$\partial_t S_\mu + \partial_\nu I_{\mu\nu} = g\mu_B \epsilon_{\mu\nu\lambda} S_\nu B_\lambda \quad (1)$$

where S_μ is the spin density, $I_{\mu\nu}$ is the spin current tensor (current of the μ^{th} component of spin running along the ν^{th} direction). Here g and μ_B are the gyromagnetic factor and Bohr magneton. In a single-channel conductor, this becomes

$$\partial_t \vec{S} + \partial_x \vec{I} = g\mu_B (\vec{S} \times \vec{B}), \quad (2)$$

where \vec{S} and \vec{I} are the spin and spin-density current. These two equations are operator identities, and hence trivially hold for the expectation values of the spin current and density, since they are linear. No assumption whatsoever is made regarding single-electron phase coherence, and indeed these would hold even in a non-degenerate electron gas at high temperature with large amounts of inelastic scattering, provided SU(2) spin-rotation symmetry is only weakly broken. Clearly then, spin precession – and associated magnetotransport oscillations – may occur even in strongly incoherent (indeed classical) media.

To elucidate the aspects of magnetotransport oscillations which *do* rely on single electron coherence, we consider a simple situation in which the classical and quantum limits can be compared and contrasted. We focus on a double barrier structure consisting of two tunneling barriers separated by a region where a magnetic field is applied perpendicularly to the system (See Fig.1). Incidentally, such Zeeman fields tailored on a mesoscopic scale have been ingeniously achieved by making use of the Overhauser effect through which optically polarized spin nuclei induce a Zeeman magnetic field on the conduction electrons through the contact interaction. In this way magnetic fields of the order of 1 Tesla extending over a range of microns have been obtained¹¹. We describe (by definition) the coherent quantum limit of this system using the Landauer-Büttiker formalism for

electron wave scattering using the S-matrices for the two barriers. The classical limit is more delicate to define. Indeed, varying degrees of decoherence can occur via different physical mechanisms, by which individual electrons interchange energy between each other or with other degrees of freedom (e.g. phonons). The exchange of energy leads to dephasing – via $d\phi/dt = E/\hbar$ – as well as energy equilibration. To maximize the contrast with the coherent case, we consider the most extreme classical limit, suggested by Büttiker^{12,13}, in which local electronic reservoirs are *attached* to the wire (see Fig. 2). These local equilibrium regions can be considered either as fictitious or real voltage probes. The randomization of the phase occurs by removing electrons from the phase coherent channels and reinjecting them without any phase relationships. Because in this approach electrons are actually interchanged between the reservoirs and the wire, not only is the single electron phase randomized but also energy and particle number are locally equilibrated. Hence, this picture can be viewed as a discrete limit of a hydrodynamic approach: while in hydrodynamics there is continuous local equilibrium at each point, in this model local equilibrium is realized only at the two points of the voltage probes.

From our calculations we find there are qualitative differences between incoherent and coherent propagation. We demonstrate that for phase coherent electrons, spin (charge) current can be generated from charge (spin) chemical potential, a situation which has no classical analog. These results can be understood in terms of quantum interference between multiple partial waves. Constructive interference between multiple reflections is determined by the added phase due to the applied magnetic field. We find that this can be put to use to create a spin valve where small changes in magnetic field lead to large changes in conductance. In the classical regime, the phase loss induced by the extra contacts obliterate the quantum interference but nevertheless spin precession arises. However, its nature is different and is to be interpreted as arising from resonances instead of quantum interferences.

The remainder of the paper is organized as follows. In Sec. II. we give a description of spin transport in the Buttiker-Landauer model and derive the magnetoconductance of a 1-d wire for coherent electron propagation. In Sec. III. we consider incoherent electron propagation and determine the spin hydrodynamic equations in the ballistic regime. The results of the two approaches are elaborated and discussed in Sec. IV. Finally, in Sec. V. we present possible experimental implementations and a summary.

II. MODEL: SCATTERING APPROACH

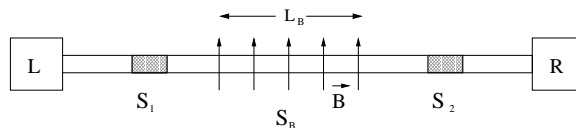


FIG. 1: Sketch of the double barrier. Spin-polarized currents are injected in the wire through the left (L) and right (R) contacts. The two potential barriers are characterized by scattering matrices S_1 and S_2 whereas the the mid-region is subject to a tunable perpendicular magnetic field whose effect can be represented by the scattering matrix S_B .

We adopt a scattering approach to treat coherent electron propagation through a double barrier, focusing for simplicity on the ballistic regime in which the elastic mean free path l_e is much larger than the channel length L_c . The corresponding formalism is based on the scattering matrix (S-matrix), which connects incoming \hat{a} and outgoing \hat{b} electron annihilation operators in the (L) left and (R) right leads, such that

$$\begin{pmatrix} \hat{b}_L \\ \hat{b}_R \end{pmatrix} = \begin{pmatrix} S_{LL} & S_{LR} \\ S_{RL} & S_{RR} \end{pmatrix} \begin{pmatrix} \hat{a}_L \\ \hat{a}_R \end{pmatrix}. \quad (3)$$

Here, we consider only two allowed propagation channels (one for each spin), so that each S_{ij} is a 2×2 spin matrix. The corresponding creation operators \hat{a}^\dagger and \hat{b}^\dagger are similarly connected by the hermitian conjugated S-matrix.

In the Landauer-Büttiker approach, the incident flow of electrons into the wire is determined by the electron distribution in the reservoirs. We consider paramagnetic contacts spin polarized along a given direction \hat{n} such that each spin band is characterized by its own Fermi-Dirac distribution¹⁴. In the proper spin basis, the occupation numbers in the contacts are given by

$$\langle a_{mi\alpha}^\dagger a_{nj\beta} \rangle = \delta_{mn} \delta_{ij} \delta_{\alpha\beta} f_\alpha(\epsilon_{mi\alpha}), \quad (4)$$

where the Fermi distribution f_α is

$$f_\alpha(\epsilon) = \frac{1}{e^{(\epsilon - \mu_\alpha)/k_B T} + 1}. \quad (5)$$

Here $a_{mi\beta}^\dagger$ and $a_{mi\beta}$ are respectively creation and annihilation electron operators in the contact $i = L/R$, with spin $\alpha = \uparrow / \downarrow$ and quantum number m representing other degrees of freedom besides the spin. The energy ϵ is the single particle excitation energy. This double Fermi distribution function is realized provided that the interactions in the contacts preserve spin, but randomize the quantum number m (e.g. the kinetic momentum). Thus the double Fermi distribution function describes two distinct (spin up and down) populations of electrons whose numbers are separately conserved but which may exchange energy and hence share the same temperature. We define a spin chemical potential $\vec{\mu}$ to be $(\mu^\uparrow - \mu^\downarrow) \hat{n}$ where \hat{n} is the direction of the spin polarization, and the charge chemical potential as $\mu = (\mu^\uparrow + \mu^\downarrow)/2$.

The spin chemical potential determines the occupations (partially traced density matrix)

$$\sum_m \langle a_{mi\alpha}^\dagger a_{mi\beta} \rangle = \delta_{\alpha\beta} N/2 + N(0) \left(\mu_i^0 \delta_{\alpha\beta} + \frac{1}{2} \vec{\mu}_i \cdot \vec{\sigma}_{\beta\alpha} \right), \quad (6)$$

where $\mu^0 = \mu - \epsilon_F$ is the charge chemical potential deviation due to electrostatic potentials, $\vec{\sigma} = (\sigma^x, \sigma^y, \sigma^z)$ are the Pauli matrices and $N, N(0)$ are the number of particles and the density of states per spin at the Fermi energy respectively. Note that the spin polarization is related to the spin chemical potential via $\vec{S} = N(0)\vec{\mu}/2$. We emphasize that this is a different situation than the case of ferromagnetic contacts, in which the majority and minority carriers share the same chemical: the spin chemical potential vanishes and the spin polarization is due to a non-zero internal exchange field. Experimentally, a non-vanishing spin chemical potential can be realized in electron-doped III-V semiconductors by optical methods which highly polarize the doped conduction band¹⁵. In the absence of magnetic impurities and spin orbit interaction, the spin polarization is a conserved quantity and a double Fermi distribution is achieved. Hence, this distribution can be realized for times larger than the inelastic scattering time, to allow for thermalization of each spin specie, but smaller than the spin-flip scattering time in order to preserve the spin polarization.

According to Landauer, the charge I^0 and spin \vec{I} currents in the lead i can be written as

$$I_i^0 = e \sum_\alpha \sum_m v_{mi} \left(\langle a_{mi\alpha}^\dagger a_{mi\alpha} \rangle - \langle b_{mi\alpha}^\dagger b_{mi\alpha} \rangle \right) / L, \quad (7)$$

$$\vec{I}_i = \frac{\hbar}{2} \sum_{\alpha\beta} \sum_m v_{mi} \left(\langle a_{mi\alpha}^\dagger \vec{\sigma}_{\alpha\beta} a_{mi\beta} \rangle - \langle b_{mi\alpha}^\dagger \vec{\sigma}_{\alpha\beta} b_{mi\beta} \rangle \right) / L, \quad (8)$$

where v_{mi} is the velocity of the level m in the lead i along the x -direction and L is the length of the wire. Note from hereon we will make use of the fundamental units where $\hbar = 1$ and $e = 1$. We use the convention that the incoming currents are positive. For small chemical potential (relative to the Fermi energy), we can consider the scattering matrix to be energy-independent. In the zero-temperature limit, we arrive to the current equations

$$\begin{aligned} I_i^0 &= \frac{1}{2\pi} \left\{ 2\mu_i^0 - \sum_{j=R,L} \left(\mu_j^0 \text{Tr}[S_{ji}^\dagger S_{ij}] + \frac{\vec{\mu}_j}{2} \cdot \text{Tr}[\vec{\sigma} S_{ji}^\dagger S_{ij}] \right) \right\}, \\ \vec{I}_i &= \frac{1}{4\pi} \left\{ \vec{\mu}_i - \sum_{j=R,L} \left(\mu_j^0 \text{Tr}[S_{ji}^\dagger \vec{\sigma} S_{ij}] + \sum_\nu \frac{\mu_j^\nu}{2} \text{Tr}[\sigma^\nu S_{ji}^\dagger \vec{\sigma} S_{ij}] \right) \right\}. \end{aligned} \quad (9)$$

We note that the spin (charge) chemical potential can also generate charge (spin) current. Also one can readily check that these equations are gauge invariant, i.e. a uniform shift of the charge chemical potentials does not generate any currents. We also emphasize that due to the mode coupling term in Eq. 1, the spin current need not be the same in both leads. This is contrast to the charge current where charge conservation implies that $I_L^0 = -I_R^0$.

To derive an explicit expression for the entire scattering matrix S of the system, we first describe the effect of the potential barriers S_1 and S_2 sketched in Fig. 1 by using the most general spin-independent scattering matrices for a two-channel system,

$$S_j = e^{i\eta_j} \left[i e^{i\xi_j \tau^z} \sin(\gamma_j) + \tau^x \cos(\gamma_j) \right] \otimes \sigma^0, \quad (10)$$

where $\tau^0, \vec{\tau}$ are the 2×2 identity and Pauli matrices respectively acting in the basis of incoming and outgoing electrons. Each barrier transmits and reflects electrons with probability $T_j = \cos^2(\gamma_j)$ and $R_j = \sin^2(\gamma_j)$, respectively. The overall phase η_j is merely a propagating phase for all processes and without loss of generality will be set to zero from now on. The phase ξ_j introduces an asymmetric phase shift between the backscattering of electrons coming from the left and the right.

We also ascribe a scattering matrix to the spin precession generated by the magnetic field in the double barrier region. For a Zeeman field pointing along the z -direction, the spin-dependent phase winding yields

$$S_B = \tau^x \otimes \exp(i\delta\sigma^0 - i\theta\sigma^z/2), \quad (11)$$

where $\delta = k_F L'$ and $\theta/2 = g u_B B^z L_B / 2 v_F$ are respectively the quantum mechanical phase acquired by free electrons propagating over an interbarrier distance L' , and the spin-dependent phase due to the winding in the magnetic field over a length L_B . Here g, u_B, B^z, v_F, k_F are respectively the gyromagnetic ratio, the Bohr magneton, the magnetic field, the Fermi velocity and the Fermi wavevector. Physically, the electron spins undergo a rotation by an angle θ in the $x - y$ plane upon crossing the magnetic field region. The S-matrix of the entire system is obtained by considering the combined effects of the potential barriers S_1, S_2 and the phase winding S_B and summing over all possible electron paths. Although we have determined the full scattering matrix, for ease of presentation we will set $\xi_1 = \xi_2 = 0$ and $\gamma_1 = \gamma_2 = \gamma$ to obtain the total S-matrix

$$S = \frac{1}{\sigma^0 + \sin^2(\gamma) e^{i(2\delta\sigma^0 - \theta\sigma^z)}} \{ i\tau^0 \sin(\gamma) \otimes [\sigma^0 + e^{i(2\delta\sigma^0 - \theta\sigma^z)}] + \tau^x \cos^2(\gamma) \otimes e^{i(\delta\sigma^0 - 1/2\theta\sigma^z)} \}. \quad (12)$$

The denominator is a result of multiple reflections between the two barriers. Notice that S is periodic with respect to θ with a period of 4π which corresponds to two complete spin rotations. Substituting the scattering matrix into Eq. (9), we obtain the charge and spin currents in the two leads:

$$\begin{aligned} I_L^0 &= \frac{T^2}{2\pi} \left(\frac{1}{|\Delta_1|^2} + \frac{1}{|\Delta_2|^2} \right) (\mu_L^0 - \mu_R^0) + \frac{T^2}{4\pi} \left(\frac{1}{|\Delta_1|^2} - \frac{1}{|\Delta_2|^2} \right) (\mu_L^z - \mu_R^z), \\ I_L^x &= \frac{1}{4\pi} \left[\mu_L^x - 4(1-T) \cos\left(\frac{\theta}{2} - \delta\right) \cos\left(\frac{\theta}{2} + \delta\right) \text{Re} \left(\frac{\mu_L^x + i\mu_L^y}{\Delta_1^* \Delta_2} \right) - T^2 \text{Re} \left(\frac{\mu_R^x + i\mu_R^y}{\Delta_1^* \Delta_2} \right) \right], \\ I_L^y &= \frac{1}{4\pi} \left[\mu_L^y - 4(1-T) \cos\left(\frac{\theta}{2} - \delta\right) \cos\left(\frac{\theta}{2} + \delta\right) \text{Im} \left(\frac{\mu_L^x + i\mu_L^y}{\Delta_1^* \Delta_2} \right) - T^2 \text{Im} \left(\frac{\mu_R^x + i\mu_R^y}{\Delta_1^* \Delta_2} \right) \right], \\ I_L^z &= \frac{T^2}{8\pi} \left(\frac{1}{|\Delta_1|^2} + \frac{1}{|\Delta_2|^2} \right) (\mu_L^z - \mu_R^z) + \frac{T^2}{4\pi} \left(\frac{1}{|\Delta_1|^2} - \frac{1}{|\Delta_2|^2} \right) (\mu_L^0 - \mu_R^0), \end{aligned} \quad (13)$$

where $\Delta_{1/2} = \exp(-i\delta \pm i\theta/2) + (1-T) \exp(i\delta \mp i\theta/2)$. The currents in the right lead can be simply obtained by performing the transformation $R \leftrightarrow L$. From the current formula, we can read off that the spin currents in the $x - y$ plane (I^x, I^y) depend only on the in-plane spin chemical potentials μ^x, μ^y , whereas the charge current I^0 and the spin current I^z depend on μ^0, μ^z . This result can be traced back to the fact that the scattering matrix does not have off diagonal elements in the spin basis, so that the spin up and down currents in the z -basis are separately preserved. Since the currents I^0 and I^z are respectively a sum and a difference of these currents, this explains why I^0 and I^z are proportional to the difference of chemical potentials in each lead. It is interesting to notice that it is possible to drive a spin(charge) current by an electrostatic(spinn) chemical potential. This situation has no classical analog, as we will see below.

III. CLASSICAL PROPAGATION

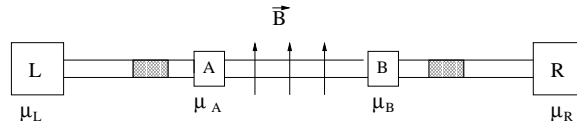


FIG. 2: Sketch of the double barrier system. Spin chemical potential is applied on the left (L) and right (R) contacts. The two voltage probes A and B randomize the phase of the injected electrons and destroy the effects of quantum coherence

In general, we expect differences from the above results, derived assuming coherent electron propagation, when a single electron's phase is significantly scrambled in the time required to propagate between the two barriers. As discussed in the introduction, in this section we consider an extreme classical limit, in which not only is this single electron phase coherence completely lost, but also the electrons are allowed to locally equilibrate inside the structure, at the locations of the voltage probes A and B (with chemical potentials μ_A, μ_B) in Fig. [2]. Such local equilibrium is in general required to achieve fully classical behavior, e.g. Ohm's law for charge conduction.

Assuming the effect of scattering by the barriers can be modeled classically (on distances longer than the length of the barriers but smaller than the inter-barrier distance), we may determine the spin current using the continuity equation, Eq. (2), and the classical hydrodynamic equation,

$$\partial_t \vec{I} + v_F^2 \partial_x \vec{S} = -g\mu_B (\vec{I} \times \vec{B}) - \vec{I} / \tau_{el}^s \quad (14)$$

where τ_{el}^s is the relaxation time for spin currents, which we assume to be governed by the elastic collision time. We assume $\tau_{\text{el}}^s \neq 0$ only within the regions of the barriers. Then in the steady state, Eq. (2) implies \vec{I} is constant through each barrier, and integrating Eq. (14) through the barrier regions gives

$$\begin{aligned}\vec{I}_L &= \frac{v_F \tau_{\text{el}}^s}{2\pi L_{\text{bar}}} (\vec{\mu}_L - \vec{\mu}_A), \\ \vec{I}_R &= \frac{v_F \tau_{\text{el}}^s}{2\pi L_{\text{bar}}} (\vec{\mu}_R - \vec{\mu}_B),\end{aligned}\quad (15)$$

where L_{bar} is the length of the contact. Comparing with the Landauer-Büttiker result for the spin conductance of a single barrier, we will take $\frac{v_F \tau_{\text{el}}^s}{2\pi L_{\text{bar}}} = T/4\pi$ in the following. Similarly solving Eqs. (2,14) in the region between A and B gives

$$\begin{aligned}\vec{I}_L &= \frac{1}{4\pi} (\vec{\mu}_A - \hat{R}_\theta \vec{\mu}_B), \\ \vec{I}_R &= \frac{1}{4\pi} (\vec{\mu}_B - \hat{R}_\theta \vec{\mu}_A),\end{aligned}\quad (16)$$

where, in the (x, y, z) basis, \hat{R}_θ reads

$$\hat{R}_\theta = \begin{pmatrix} \cos(\theta) & -\sin(\theta) & 0 \\ \sin(\theta) & \cos(\theta) & 0 \\ 0 & 0 & 1 \end{pmatrix}.\quad (17)$$

The similar but more trivial classical result for the charge currents is

$$\begin{aligned}I_L^0 &= \frac{T}{\pi} (\mu_L^0 - \mu_A^0) = \frac{1}{\pi} (\mu_A^0 - \mu_B^0), \\ I_R^0 &= \frac{T}{\pi} (\mu_R^0 - \mu_B^0) = \frac{1}{\pi} (\mu_B^0 - \mu_A^0).\end{aligned}\quad (18)$$

Solving these Kirchoff's-like equations for the spin chemical potentials $\vec{\mu}_A$ and $\vec{\mu}_B$ of the reservoirs A and B, we find

$$\begin{pmatrix} \vec{\mu}_A \\ \vec{\mu}_B \end{pmatrix} = \hat{K} \begin{pmatrix} 1+T & \hat{R}_\theta \\ \hat{R}_\theta & 1+T \end{pmatrix} \begin{pmatrix} \vec{\mu}_L \\ \vec{\mu}_R \end{pmatrix}\quad (19)$$

as well as the currents:

$$I_L^0 = -I_R^0 = \frac{1}{\pi} \frac{T}{2+T} (\mu_L^0 - \mu_R^0)\quad (20)$$

$$\begin{pmatrix} \vec{I}_L \\ \vec{I}_R \end{pmatrix} = \frac{1}{4\pi} \left[T \hat{K} \begin{pmatrix} 1+T & \hat{R}_\theta \\ \hat{R}_\theta & 1+T \end{pmatrix} \begin{pmatrix} \vec{\mu}_L \\ \vec{\mu}_R \end{pmatrix} + \begin{pmatrix} T & 0 \\ 0 & T \end{pmatrix} \begin{pmatrix} \vec{\mu}_L \\ \vec{\mu}_R \end{pmatrix} \right].\quad (21)$$

Here we defined

$$\begin{aligned}\hat{K} &= T[\hat{R}_\theta^2 - \hat{I}(1+T)^2]^{-1} \\ &= \frac{T}{1 + (1+T)^4 - 2(1+T)^2 \cos(2\theta)} \begin{pmatrix} \cos(2\theta) - (1+T)^2 & \sin(2\theta) & 0 \\ -\sin(2\theta) & \cos(2\theta) - (1+T)^2 & 0 \\ 0 & 0 & -\frac{1+(1+T)^4 - 2(1+T)^2 \cos(2\theta)}{T(2+T)} \end{pmatrix}\end{aligned}\quad (22)$$

and \hat{I} is the 3×3 identity matrix. For weak tunneling ($T \ll 1$), the matrix \hat{K} is responsible for the resonances in the current function. Note that in addition to dephasing, each reservoir randomized the electronic momentum and generated an additional resistance. This extra resistance can be read off from the charge current where the total transmission trough the system is given by the fraction $\frac{T}{2+T} < 1$, to be compared to the result for coherent electrons $\frac{T}{2-T}$. The former can be written as $(\frac{2R}{T} + 1)^{-1}$ whereas the latter is $(\frac{2R}{T} + 1 + 2)^{-1}$. For coherent propagation the resistance is the sum of $\frac{2R}{T}$ corresponding to the intrinsic resistance of the potential barriers and 1, the quantum resistance associated to the left and right contacts. In the case of incoherent propagation, there is an additional factor of 2 due to the quantum resistances of the two voltage probes.

IV. DISCUSSION

A. Low transmission limit

Phase coherence is known to affect transport properties in the charge channel. However, much less is known in the spin sector. One may expect that these differences, if present, to be enhanced in the low transmission limit where multiple reflections in the intrabARRIER region occurs. In this problem, we first point out that in the case of incoherent propagation spin and charge are completely decoupled, i.e., classically the spin chemical potential cannot give rise to charge current and vice versa. The charge conductance and spin conductance along the z -axis are given by $G_c = \frac{1}{\pi} \frac{T}{2+T}$ and $G_s^z = \frac{1}{4\pi} \frac{T}{2+T}$ respectively. In the geometry investigated, the Zeeman magnetic field does not exert any force on the z component of the spin or on the electric charge, therefore the spin and charge are separate conserved quantities and each has an associated conductance that is independent of the applied magnetic field. However, for coherent electron propagation, spin and charge mix as shown in Eq. (13). This effect is due to the filtering action of the magnetic field. In the low transmission limit the tunneling transmission is strongly enhanced for specific values of the applied magnetic field (see Fig.4). This can be explained on the basis of constructive interference between multiple electron wave reflections at the scattering barriers. Analyzing Eq. (12), this condition translates for an electron with spin $\uparrow / \downarrow = + / -$ as $(2\delta \pm \theta + \pi = 2\pi n)$. Hence, the spin current is periodic with respect to θ with a period of 2π , and the different peaks corresponds to constructive interference for spin up and down electrons. In the limit $T \rightarrow 0$, the charge and spin currents at the resonant values are

$$\begin{aligned} I_L^0 &= \frac{1}{2\pi}(\mu_L^0 - \mu_R^0) \pm \frac{1}{4\pi}(\mu_L^z - \mu_R^z), \\ I_L^z &= \frac{1}{8\pi}(\mu_L^z - \mu_R^z) \pm \frac{1}{4\pi}(\mu_L^0 - \mu_R^0), \end{aligned} \quad (23)$$

while the currents in the right lead are obtained by interchanging L and R .

For simplicity in Fig.4 we depict only the currents in the left lead I_L^0, I_L^z in the case of the only non-zero applied chemical potential $\mu_L^z - \mu_R^z = 1$. In this geometry, a double barrier system can be seen as a spin valve where a small deviation in the magnetic field from the constructive interference condition lead to a large change in conductance. Also we notice that, since the charge and the spin are carried by the same particle, a positive (negative) charge current is also generated when a spin up (down) is transmitted. Hence, this phenomenon is essentially linked to the particle/wave duality of the electron.

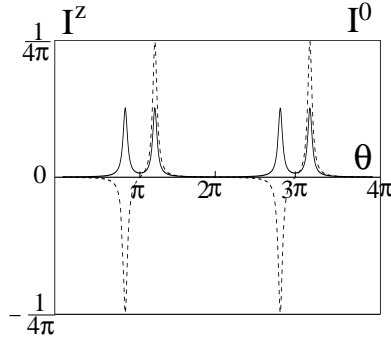


FIG. 3: Charge current I^0 in dash line and z -spin current I^z shown by the solid curve for fully coherent tunneling. A spin chemical potential $\mu_L^z - \mu_R^z = 1$ is applied, leading to a non-zero charge current. We took $T = 0.1$ and $\delta = 0.3$.

To further illustrate and contrast the results of Eqs. (13) and (20-21), we present results for the spin current in the presence of spin chemical potentials along the x or y axis. Classically, the spin would merely precess in the $x - y$ plane due to the magnetic field. A strong transmission occurs when spins perform a complete revolution upon a closed trajectory between the barriers, i.e. the acquired phase $2\theta = 2n\pi$, and the partial spin reflections are added in phase giving rise to a spin resonance. If the spins precess by $\theta = 2k\pi$ respectively $(2k + 1)\pi$ while traveling from one potential barrier to the other the transmitted spin current in the right lead points along the positive, respectively negative x direction as depicted in Fig. 5. The value of the currents at such resonances are

$$I_L^x = \frac{1}{4\pi} \frac{T}{2+T} (\mu_L^x \pm \mu_R^x) \quad (24)$$

$$I_L^y = \frac{1}{4\pi} \frac{T}{2+T} (\mu_L^y \pm \mu_R^y) \quad (25)$$

where the \pm signs correspond to resonances at $\theta = 2k\pi, (2k+1)\pi$ respectively and the currents in the right lead are determined as usual by interchanging the L and R symbols. Far off resonance, the spins are added out of phase and a small current of order T^2 is generated. On the other hand, for fully coherent electrons, the current peaks do not occur upon full spin revolutions in the barrier but, as mentioned earlier, are determined by the constructive interference between multiple partial waves. Interestingly, as shown in Fig. 3, we point out that the spin current in the left lead points along the y axis for broad ranges of the applied magnetic field. It is also straightforward to show that in this case (i.e. $\mu_L^x \neq 0$), at the points of constructive interference, the ratio of spin currents in the right lead is

$$\frac{I_R^x}{I_R^y} = \frac{1-R}{1+R} \cot(\theta). \quad (26)$$

Hence in the low transmission limit, the spin currents emerge with a spin direction mostly along the y axis. It is worth emphasizing that even if one considers all phase factors in the potential barriers (Eq. (10)) the result remains unchanged and is consequently a robust prediction.

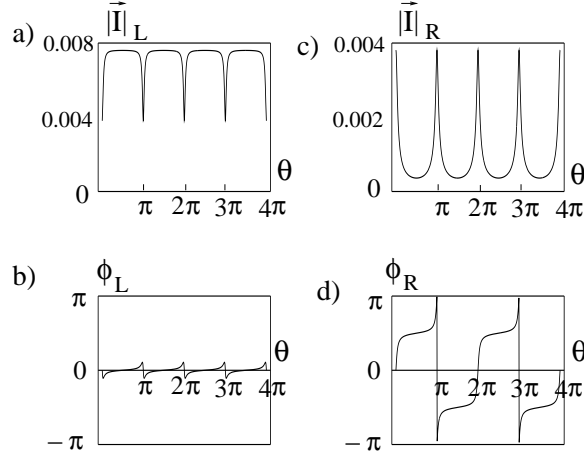


FIG. 4: Incoherent propagation for opaque barriers: The magnitude and the direction in the xy plane of the spin current in the left (L) and right (R) leads respectively as a function of θ . A spin chemical potential $\mu_L^x = 1$ is applied on the left lead. The transmission $T = 0.1$

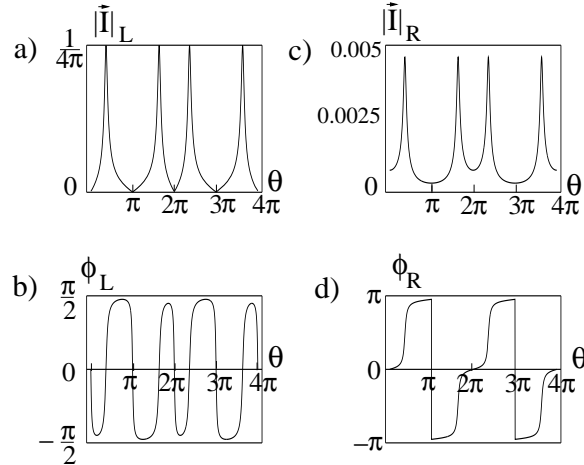


FIG. 5: Coherent propagation for opaque barriers: The magnitude and the direction in the xy plane of the spin current in the left and right leads respectively as a function of θ . The transmission $T = 0.1$ and $\mu_L^x = 1$.

B. High transmission limit

Most of our discussion is focused on the limit of low transmission of the barriers when the most important effects are due to resonant tunneling through the two barriers. Hence, in the high transmission limit, electrons impinging on the potential barriers are most likely to be transmitted, therefore one expects the interference effect resulting from the multiple reflections to be reduced. Restricting our attention to perfectly transmitting barriers ($T = 1$), we find the currents in the phase-coherent regime to be given by

$$\vec{I}_L = \frac{1}{4\pi}(\vec{\mu}_L - \hat{R}_\theta \vec{\mu}_R).$$

Hence the currents are precessing in the magnetic field following Eqs. (14) as one might have expected. However, this is to be contrasted with the behavior in the phase incoherent regime,

$$\begin{pmatrix} I_L^x \\ I_L^y \\ I_L^z \end{pmatrix} = \frac{1}{4\pi} \frac{1}{8 \cos(2\theta) - 17} \begin{pmatrix} -9 + 6 \cos(2\theta) & -2 \sin(2\theta) & 0 \\ 2 \sin(2\theta) & -9 + 6 \cos(2\theta) & 0 \\ 0 & 0 & (8 \cos(2\theta) - 17) / 3 \end{pmatrix} \begin{pmatrix} \mu_L^x \\ \mu_L^y \\ \mu_L^z \end{pmatrix} \quad (27)$$

$$+ \frac{1}{4\pi} \frac{1}{8 \cos(2\theta) - 17} \begin{pmatrix} 3 \cos(\theta) & -5 \sin(\theta) & 0 \\ 5 \sin(\theta) & 3 \cos(\theta) & 0 \\ 0 & 0 & -(8 \cos(2\theta) - 17) / 3 \end{pmatrix} \begin{pmatrix} \mu_R^x \\ \mu_R^y \\ \mu_R^z \end{pmatrix}. \quad (28)$$

The unexpected difference between the two previous results is linked to the extra resistance introduced by the voltage probes A and B , as discussed in section II. The voltage probes achieve phase randomization by bringing in local equilibrium at the point of contact. Although inelastic scattering is needed to implement decoherence, the Büttiker dephasing model enforces the more stringent condition of local equilibrium. The momentum randomization affects both the transmitted and reflected current which show extra oscillations with the magnetic field due to the backscattering of the electrons.

V. HYDRODYNAMICS, EXPERIMENTAL IMPLEMENTATION AND CONCLUSIONS

From the above discussion, it is apparent that there are numerous features distinguishing the classical precessional limit from truly single electron phase coherent propagation. Hence in analyzing experiments, it is important to distinguish the various time scales being measured, e.g. the phase coherence time τ_ϕ beyond which classical behavior obtains from τ_s , beyond which magnetization relaxes and all signs of precession are lost (precession can also be destroyed experimentally by other means, e.g. inhomogeneous magnetic fields characterized by T_2 times). The identifying of the various scattering times – other than τ_ϕ which is determined by the loss of true interference phenomena – should be made by their definitions through hydrodynamic equations. Such equations generalize Eqs. (2,14), whose utility is emphasized by the simplicity of the classical calculations in Sec. III. In hopes that such careful determinations of various time scales may be made, we give the hydrodynamics appropriate for electrons in III-V semiconductors, including the possibly important effects of Rashba interactions due to electron confinement. For a one-dimensional wire, the equations yield

$$\begin{aligned} \partial_t \vec{S} + \partial_x \vec{I} &= -\frac{\vec{S}}{\tau_s} + g\mu_B \vec{S} \times \vec{B} + \frac{\alpha_R m^*}{\hbar^2} (\vec{I} \times \hat{Q}), \\ \partial_t \vec{I} + v_F^2 \partial_x \vec{S} &= -\frac{\vec{I}}{\tau_{el}^s} - \frac{e}{m^*} E_x \vec{S} - g\mu_B \vec{I} \times \vec{B} + \frac{v_F^2 \alpha_R m^*}{\hbar^2} (\vec{S} \times \hat{Q}) - \frac{g\mu_B \hbar n}{4m^*} \partial_x \vec{B} - \frac{u}{\hbar} \vec{S} \times \vec{I} \end{aligned} \quad (29)$$

where α_R is the Rashba coefficient, \hat{Q} is the direction of the Rashba spin-splitting, E_x is the bias electric field, n is the electron number density and τ_s is the spin relaxation time. The last term with coefficient $u \sim e^2 k_F$ derived from the electron-electron interaction yield non-linear equations which severely complicate the solution¹⁶. However, we emphasize that on general ground, any spin dependent interaction, such as the Rashba interaction, can lead to spin oscillations. In the single electron phase coherent propagation, the spin transport is determined by the quantum interference between partial waves, the magnetoconductance due to a Rashba interaction is also expected to differ from the classical regime although the details need to be worked out.

Now, we return to the simple situation discussed in this paper and address the question of experimental feasibility. To realize coherent ballistic precession, the length of the device must be long enough to allow for a full spin revolution in the double-barrier region but short enough for electrons to propagate coherently and ballistically. Magnetic fields of 1 Tesla set the former limit to lengths larger than $1\mu m$. On the other hand, mean free paths in excess of $10\mu m$ have been achieved in clean semiconductor

heterojunctions. Non-zero temperature will lead to decoherence due to phonons interaction. Moreover, because the interference phenomena depend crucially on the phase accumulated between the two barriers, the phase accumulated by the two *longitudinal* modes in the absence of a magnetic field should be much smaller than 2π . This also sets a limit for the temperature operation range and spin chemical potential to be less than $\hbar L/v_F \approx 10K$. Above this energy scale, thermal broadening and energy dependent tunneling elements would obliterate the quantum interference. Another experimental challenge is the measurement of the spin currents. Here we suggest that spin currents be obtained through measuring the spin polarization of the contacts. Indeed, in the absence of magnetic forces, the spin being conserved, the flow of spin into the contacts can be related to the time-dependent spin polarization of the contact ($I^\nu = \partial_t S^\nu$). In conclusion, we have analyzed spin transport in double barrier system in the phase coherent and incoherent regimes. We showed that for coherent propagation, the standard Boltzmann equations for spin transport do not capture the rich behavior which can however be understood in terms of quantum interference between multiple wave reflections. While completing this paper, we became aware of the work of Mireles *et al.*¹⁷ on spin injection in the quantum coherent regime where similar conclusion were reached.

Acknowledgments

This work was supported by the NSF through grant DMR-9985255, and the Sloan and Packard foundations.

* Electronic address: veillet@physics.ucsb.edu

† Electronic address: cristina@physics.ucsb.edu

‡ Electronic address: balents@physics.ucsb.edu

¹ S. Datta and B. Das, Appl. Phys. Lett. **56**, 665 (1990).

² D.D. Awschalom, D. Loss and D. Samarth, *Semiconductor Spintronics and Quantum Computation*, Springer Berlin, (2002) and references therein.

³ J.M. Kikkawa, I.P. Smorchkova, N. Samarth and D.D. Awschalom, Science **277**, 1284 (1997)

⁴ J.M. Kikkawa and D.D. Awschalom, Phys. Rev. Lett. **80**, 4313 (1998).

⁵ T. Valet and A. Fert, Phys. Rev. B **48** 7099 (1993).

⁶ M. Johnson, Phys. Rev. B **58**, 9635, (1998)

⁷ M. Johnson, Science **260**, 320 (1993).

⁸ F.J. Jedema, A.T. Filip, B.J. van Wess, Nature **410**, 345 (2001).

⁹ S. Datta, *Electronic Transport in Mesoscopic Systems*, Cambridge University Press, Cambridge, (1995).

¹⁰ I. Yoseph, *Introduction To Mesoscopic Physics*, Oxford University Press (1997).

¹¹ J.M. Kikkawa and D.D. Awschalom, Science, **287**, 473 (2000); R. K. Kawakami et. al., Science, **294**, 131 (2001).

¹² M. Büttiker, Phys. Rev. **B33**, 3020 (1986); IBM J. Res. Dev. **32**, 63 (1988).

¹³ I. Knittle, F. Gagel and M. Schreiber, Phys. Rev. B. **60**, 916 (1999).

¹⁴ H.X. Tang et al. in *Semiconductors Spintronics and Quantum Computation*, edited by D.D. Awschalom, D. Loss, N. Samarth, Springer Berlin,(2002).

¹⁵ I. Malajovich, J.M. Kikkawa, D.D. Awschalom, J.J. Berr, N. Samarth, Phys. Rev. Lett. **84**, 1015 (2000).

¹⁶ C. Bena and L. Balents Phys. Rev. B **65**, 115108 (2002).

¹⁷ F. Mireles and G. Kirczenow, cond-mat/0210391